INL/CON-22-69999-Revision-0

Use of Sensors and Machine Learning for Signal Discovery in a Solvent Extraction Process 23280

March 2023

Edna S Cardenas, Cody McBroom Walker, Mitchell Greenhalgh, Luis A Ocampo Giraldo, Jay D Hix, James T Johnson, Katherine Neis Wilsdon

Changing the World's Energy Future

Idaho National Laboratory

INL is a U.S. Department of Energy National Laboratory operated by Battelle Energy Alliance, LLC

INL/CON-22-69999-Revision-0

Use of Sensors and Machine Learning for Signal Discovery in a Solvent Extraction Process 23280

Edna S Cardenas, Cody McBroom Walker, Mitchell Greenhalgh, Luis A Ocampo Giraldo, Jay D Hix, James T Johnson, Katherine Neis Wilsdon

March 2023

Idaho National Laboratory
Idaho Falls, Idaho 83415

http://www.inl.gov

Prepared for the
U.S. Department of Energy
Under DOE Idaho Operations Office
Contract DE-AC07-05ID14517

Use of Sensors and Machine Learning for Signal Discovery in a Solvent Extraction Process – 23280

E. S. Cárdenas*, C. M. Walker*, M. R. Greenhalgh*, L. A. Ocampo Giraldo*, J. D. Hix*, J. T. Johnson*, K. N. Wilsdon*, and Kelly Truax**
* Idaho National Laboratory, 1955 N Fremont Ave., Idaho Falls, ID, 83415, USA
** University of Hawai'i at Manoa, Honolulu, HI 96822

ABSTRACT

Reprocessing is an important step in the nuclear fuel cycle where usable nuclear materials are extracted from used fuel for recycling. The separation of materials for reuse simultaneously reduces not only the volume of nuclear waste, but its decay time to radioactivity levels similar to that of the originating uranium ore. As part of an initiative to steward research, development, and innovation into the nuclear fuel cycle, Idaho National Laboratory is designing and constructing a solvent extraction testbed named Beartooth. This testbed will allow researchers to refine separation processes, test innovative extraction processes, and give early career scientists opportunities to gain skills in performing separations chemistry utilizing centrifugal contactors. In addition, the Beartooth testbed is being uniquely designed to enable novel technologies including machine learning capabilities for the characterization of chemical process operations in near real-time. To aid in the design of Beartooth, a team of researchers are installing a variety of atypical sensors into a system of contactors for signal discovery. The team will implement machine learning methods on acquired sensor data to extract signal features. The goal is to provide a process operator with a deeper understanding of the chemical process and equipment usage. This work will summarize sensors utilized and preliminary results from an infrared camera.

INTRODUCTION

In the nuclear industry solvent extraction and in particular the PUREX process has been extensively used for the recovery of uranium and plutonium from dissolved irradiated nuclear fuel [1-3]. Although, the recovery of plutonium greatly reduces the radiotoxicity, the minor actinides remaining in the waste are also long-lived and increase the complexity of storage [3-5]. On-going developments have led to advances in the PUREX process and alternate solvent extraction processes towards the recovery of the long-lived radionuclides with the intention of reducing the radiological risk of the waste stream [5-12]. The purity of the recovery stream as well as the radiological risk of the waste is typically determined by off-line laboratory analysis subsequent to separation activity and therefore comes with a time delay [13]. Knowledge of the concentration of chemical components in solution streams allows an operator to increase their awareness and control of a separation. Monitoring the solution concentration on-line using Raman spectroscopy, and visible and near-infrared (NIR) absorbance has been studied with all showing promising results in measuring concentrations and elements in the solution streams [14-16]. Nuclear waste streams in particular are complex and diverse therefore, efforts are ongoing towards successful on-line monitoring methods. Additional studies have shown that using machine learning (ML) implemented on the combination of measurements from Raman, NIR, and physicochemical data improves concentration accuracy [17]. The intention of this work is to complement ongoing efforts by evaluating a variety of ML approaches on data collected from a variety of disparate sensors. Although measuring the concentration is of great importance in the characterization of the process streams, this work will also look at signals that could potentially inform a process operator of various operational events. The addition of sensors that measure equipment usage has the potential to inform an operator of process progress and may help to identify anomalous activities such as leaks in the system as well as aiding in the prediction of equipment faults and failures. These types of activities have the potential to increase an operator's knowledge and control of a separation which could ultimately improve the quality of that separation.

To facilitate a process operator's knowledge and increase their understanding of separation science related to the nuclear fuel cycle, Idaho National Laboratory is designing and constructing the Beartooth testbed. This testbed will provide infrastructure for separation scientists to refine flowsheets (a group of

process steps and conditions based on mass conservation and thermodynamic equations), test novel separation techniques, and give early career researchers opportunities to have hands-on experiences [18]. The testbed will reside at the Fuel Conditioning Facility at INL and be equipped with glovebox lines, dissolution equipment, and separations equipment including centrifugal contactors. Centrifugal contactors are used to initially mix two immiscible liquids, an organic and an aqueous liquid. A separation process proceeds through a series of stages with the materials of interest selectively segregated into the organic phase using an extractant [18, 19]. The denser phase of the mixed fluids is pushed to the outside of the contactor's separation zone through centrifugal forces. Ideally unwanted segregated materials can be selectively back-extracted using reducing agents [19]. At present, Beartooth is being designed to include forty centrifugal contactors. In addition, it is being designed to allow for the installation of various disparate sensors, data acquisition equipment, and internal data networking equipment. These infrastructure and equipment will enable ML capabilities that allow for the characterization of process events, solution streams, and equipment operation.

To inform in the design of Beartooth this research will install a variety of atypical sensors and develop a multi-sensor data acquisition system into a prototype solvent extraction system. The prototype solvent extraction system is similar in design to that planned for Beartooth; however, it is solely used for the separation of nonradioactive materials. A typical solvent extraction system includes sensors that track flow rate, solution temperature, and the number of revolutions per minute (RPM) of the operating contactor motors. As mentioned, research is ongoing in on-line monitoring using Raman, visible, and NIR sensors. This work will deploy atypical sensors i. e. those not traditionally used, into the prototype system for signal discovery. Sensors that are being studied for this work include those that measure vibration, acoustics, solution color, solution density, solution level, among others. The system will implement ML algorithms on the collected data to extract signal features with the goal of identifying equipment usage, process events, and solution characteristics. The objective is to determine which sensors provide relevant information singularly or when analyzed in combination would improve an operator's capability to make decisions in near real-time. The analysis will determine if signal features and/or ML methods can aid in the prediction of equipment failures, detect normal operations, and detect abnormal operations such as material leaks and/or diversion. This paper will summarize sensors utilized and preliminary results from an infrared camera that was used to capture data of solvent extraction equipment and solutions.

SENSORS & EQUIPMENT

Studies are being conducted on a prototype solvent extraction system prior to the completion of the Beartooth testbed to aid in its design. The prototype system is not equipped for use with radioactive materials; however, it includes thirty centrifugal contactors similar to those that will be used in Beartooth. The prototype system is equipped with traditionally used sensors including those that measure the flow rate of both the organic and aqueous solution streams, the solution temperature at various locations within the separation process, the ambient temperature, and the current draw of each contactor motor. Although the RPM of the contactor motors is monitored, it is currently not logged. The currently tracked measurements are collected for this work as well as measurements collected from sensors not traditionally installed in a solvent extraction system. This work will install atypical sensors to monitor equipment vibrations, acoustic activity, seismic activity, solution density, solution viscosity, solution color, solution pH, solution conductivity, liquid tank levels, infrared thermal imaging, and temperatures in various locations within the system. The authors have prepared a separate manuscript listing the brand of sensors and their sensing range [20]. The list includes sensors currently considered for ultimate use in Beartooth; however, additional sensors will be tested in the future. The manuscript also shows sensor locations relative to a single contactor. In addition, this research is evaluating lower cost sensors that are being compared to a higher cost counterpart to determine their sensing capability.

A sophisticated data collection system has been developed to manage the large number of sensors that measure data at various sampling rates. Details of the data acquisition equipment and file management can be found in a separate document [21]. Collected data is currently analyzed off-line while sensors are being evaluated for signal discovery; however, the data collection system is being developed to integrate

into INL's Deep Lynx [22]. Deep Lynx is an open-source data warehouse that will store, aggregate and exchange data, in this case between the data collection system, ML models, and researchers [23]. Integration into Deep Lynx will allow information to reach process operators in near real-time.

DISCUSSION & METHODOLOGY

The goal of this work is to provide useful information to a process operator that will enhance their understanding and potentially optimize a chemical separation process. A well-established separation process generally follows a known flowsheet. The planned research includes evaluating signals emitted during an extraction process that follows a known flowsheet; however, initial data collection campaigns focused on monitoring equipment usage in various stages of operation without the need of a full separation. Nevertheless, the aqueous solution initially contained nitric acid while the organic feed consisted of 30% tributyl phosphate Isopar L. In addition, the aqueous solution was dyed with 10 $mg \cdot L^{-1}$ methylene blue to test the functionality of the color sensor. Initial experiments focused on various operational changes such as varying the RPM of the contactor motors and changing the flow rates of each solution.

The organic and aqueous solutions start with input feeds at opposite ends of the series of contactors. In other words, in the prototype system the organic feed will start at contactor one and end at contactor thirty and vice versa for the aqueous feed. The solutions flow through separate transparent tubing lines that originate from their respective feed streams and continue from contactor to contactor. The solution streams ultimately drain into output tanks. The rate at which the solutions flow through the system is generated by pumps that transfer each solution separately. Heaters are also integrated into the system and separately heat the organic and aqueous solutions.

Typically, at the start of a separation process, the aqueous solutions are fed through the contactors to seal the internal components prior to introducing the organic solution. If the aqueous flows are not established prior to introducing the organic solution the contactors will not operate properly. Once the aqueous flow has been established through the contactors, the organic solution can then be initiated. To aid in the operator's awareness of this process, an infrared camera was used to track the location of the aqueous solution at the start of contactor operation.

The aqueous solution was heated to 55 ˚C and images were taken of the aqueous inter-connective tubing in the contactor system. Infrared images, presented in Figure 1, clearly show the aqueous solution in the tubing, indicated by the bright orange and yellow colors, as it flowed from contactor 30 and continued through to contactor 27. The consistency of the solution flow indicates functioning equipment and no blocked lines in the camera's field of view; information that would be valuable to an operator especially in highly radioactive areas where equipment tubing may be obscured. Furthermore, the solution location would allow a system operator to know exactly when the contactors are sealed with aqueous solution, thereby mitigating a potential improper operation of the contactors.

During data collection as the aqueous solution flowed from contactor to contactor, a leak occurred at the tubing-exit of contactor 28. A leak-droplet just below the tubing is visible in the infrared image shown in Figure 2. Although process operators are trained to detect leaks, infrared video shows that the leak occurred prior to operator awareness which was reported close to fifteen minutes after the start of operation. Due to this leak event, a study was conducted to determine if a ML algorithm could detect, identify, and predict a leak.

Figure 1. Infrared images taken at the rear of the contactor system showing the aqueous solution flowing from contactor 30 to contactor 29 (left), continuing to contactors 28 and 27 (center), and flowing steadily through contactors 30-27 (right). The yellow arrows point to solution flowing through the tubing connecting the contactors.

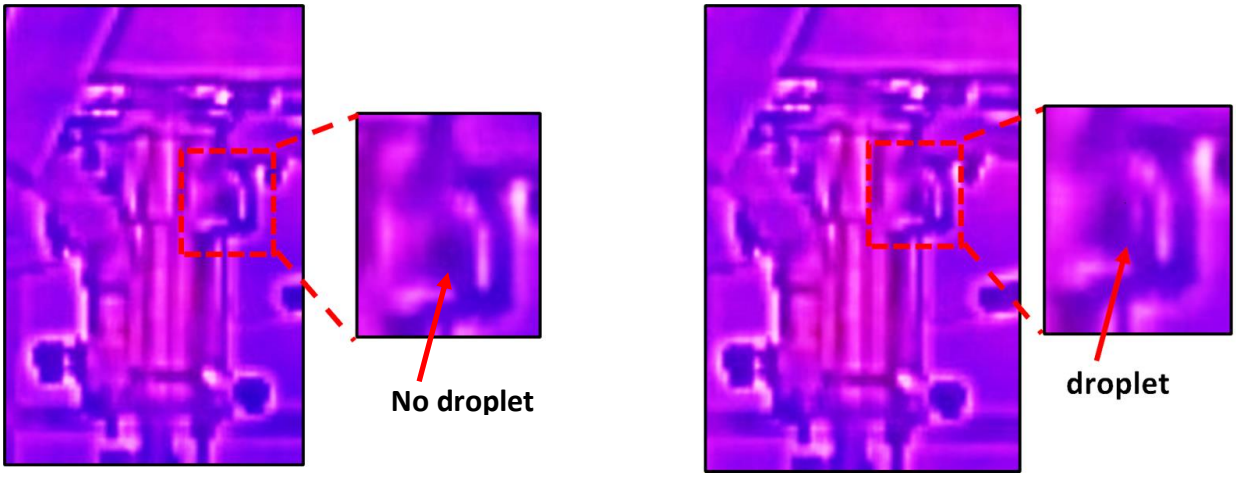

Figure 2. Infrared images showing contactor 28 without a droplet (left) and with a droplet (right) during a solution leak. The location where a droplet occurred are zoomed-in for easier visual inspection.

Images such as those presented in Figure 1 and Figure 3 were implemented into a ML algorithm to determine if an operator could be alerted of a leak prior to physical identification. Several challenges make this a difficult ML classification problem including the transients of the process as well as the dynamic changes observed between the images. Figure 3 shows the system at two different stages: before flow and when the flow was initially established. Established flow is presented in Figure 1(right). Since the leak occurred during startup, it was imperative that the ML algorithm was detecting the leak and not simply identifying the startup stage within the process. To add to this complication, the infrared images scale to the largest temperature within the camera's field of view. Because the largest temperature may change between images the color representation of temperatures within the image may also change. This makes color comparisons between images challenging. For example, before flow is established a high of 25.3°C was measured by the infrared camera, in contrast a high of 34.3°C was measured after flow was established. These high temperature values are annotated just above the color scale near the left edge of the image. The team is determining if the infrared camera can be adjusted to a fixed scale for future experiments.

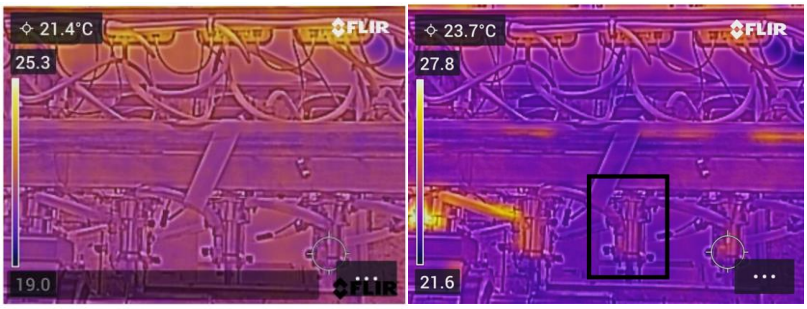

Figure 3. Infrared image at the beginning of the process before flow has begun (left). Flow is starting to be established and a leak has been identified and marked with a box (middle).

A variety of image processing techniques were applied in an effort to improve the robustness of the classification model, increase the number of training images, and to reduce overfitting. Data augmentation methods including shear (up to 20%), zoom (up to 20%), and horizontal flip were applied to the original images or following the application of image filters. Image filters included Hue-Saturation-Value (HSV), gray scale, Sobel XY, and Canny edge detection. Figure 4 shows an image segment in its original camera-output condition and after filters were applied.

The HSV filter, developed for image display on screens, combines properties (hue, saturation, value) that are more comparable to how humans generate color than the Red-Green-Blue (RGB) model [24]. In the RGB color model, red, green, and blue colors are linearly scaled on a cube, with each color representing either the length, width, or depth axes, while in the HSV model properties are scaled to a geometrical cone [25]. A determination of the hue, saturation, and value is given by the position of the color on the cone's circular dimension, the radial position, and the central vertical axis, respectively [25].

Gray scale was used as a precursor to the Sobel XY filter and converted the three-dimensional RGB color values into a one-dimensional intensity value. Gray scale was used because the rate of one-dimensional change around an object's border become more apparent than when using three-dimensional RGB values. Consequently, the Sobel edge detection algorithm used the one-dimensional rate of change (or gradient) in both the X and Y direction to determine the location of edges [26].

The Canny edge detection initially smoothed the image with a two-dimensional Gaussian operator before taking the gradient of the image [27]. A non-max suppression then determined where edges were likely based on each pixel's magnitude as related to neighboring values. A high and low threshold were then applied to determine the location of object edges [27]. If a pixel's value was above the high threshold, it was deemed an edge. If the pixel was above the low threshold and resided beside a pixel above the high threshold, then both pixels were deemed as an edge pixel. Pixels below the low threshold were never considered as edges. In Figure 4, the bottom center image (labeled as edge) used Canny edge detection to determine edges within the image. The bottom right image (labeled Threshold) used the same technique but with a lower threshold. The lower threshold allowed for more pixels to be labeled as edges.

The dataset contained one instance of a leak that occurred during the start of the separations process. Because the dataset contained time series data, images were arranged in sequential order and ultimately divided into training and validation sets. The first 85% (257 images total) of images in each class were used to train the model while the remaining 15% were reserved for validation (45 images total). The four classes were labeled startup, leakage, establishing flow, and full flow. These classes were then reduced into two classes, leak and no-leak, to allow for binary classification. Due to the low number of images within the collected dataset, augmented images were used to boost the total number of available training data (i.e., from 257 images up to 2,000) and a pre-trained model was used to boost the output performance.

The pre-trained classification model consisted of a base model, Xception, wrapped with an outer model which consisted of a GlobalAveragePooling2D layer, a dropout layer, and a dense output layer. Xception was trained on the ImageNet dataset; a large-scale dataset containing millions of annotated images [28, 29]. The Xception architecture was developed with depthwise separable convolutional layers that were linearly stacked and contained residual connections [28]. The base and outer models had 20,809,011 and 2,049 trainable parameters, respectively.

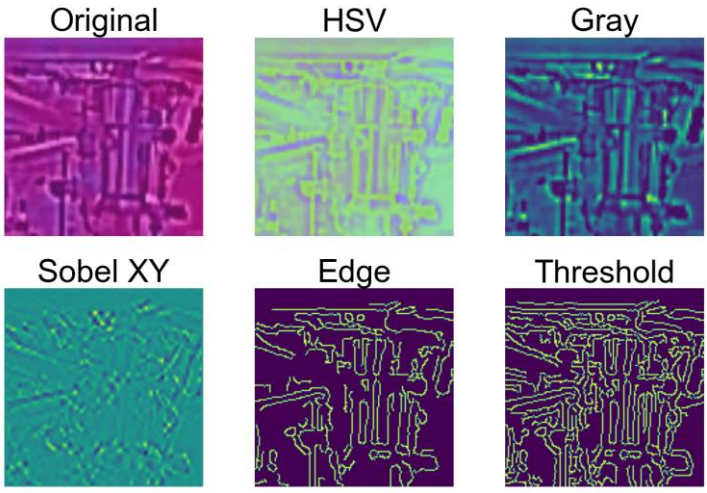

Figure 4 The original 150x150 pixel image taken with the infrared camera (top left). Original image after being converted to a Hue-Saturation-Value (HSV) color space (top center). Original image converted to gray scale (top right). The Sobel filter was applied to the gray scale image to locate edges (bottom left). Canny edge detection was implemented (bottom center). Canny edge detection with a lower threshold was implemented (bottom right).

Initially, the weights in the base model were frozen and the outer model was trained on a training dataset which contained 2,000 original and augmented (i.e., shear, zoom, flip) images. After the initial training, the weights within the base model were unfrozen and the model was trained again using the same dataset with a very low learning rate (1E-5). The process was repeated with the models trained on images in batches of four to speed up the process. This procedure allowed the classification model to be fine-tuned to the current dataset while still retaining most of the information gained from the original ImageNet dataset.

The model's classification performance was determined by the accuracy, precision, recall, and F1 score. These parameters were calculated as follows:

$$Accuracy = \frac{TP + TN}{TP + TN + FP + FN}$$

$$Precision = \frac{TP}{TP + FP}$$

$$Recall = \frac{TP}{TP + FN}$$

$$F1\ Score = 2 * \frac{Precision * Recall}{Precision + Recall}$$

where TP was the true positive, FP was the false positive, TN was the true negative, and FN was the false negative. The accuracy measured the correctly predicted observations, while the precision measured the ratio of correctly predicted positive observations to the total number of positive observations. For this paper, a positive observation meant an image with a "normal" condition i.e., no leak. The precision

informed the false positive rate and in a similar way, the recall informed the false negative rate. In addition, the F1 score took into consideration both the precision (false positive) and the recall (false negative) and was more useful than the accuracy in determining the classification performance because there were an uneven number of classes.

After classifying the images, a heatmap was generated using the fine-tuned model and Grad-CAM++. A heatmap was generated to determine the location within an image where the model was focused during its classification assessment. Grad-CAM++ assessed the gradient produced in the feature map of the last convolutional layer [30]. The intensity of the gradient was then mapped over specific feature channels and obtained the class activation heatmap. This heatmap was then overlayed on the input image to visualize where the model's prediction was determined.

RESULTS

The images, containing the leak as well as normal operating conditions, were split into training and validation datasets then augmented with filters, transformations, and other image modifiers (i.e., shear, zoom, and horizontal flip). The base model was frozen, and the outer model was trained on the training data set. Afterwards, the model was unfrozen and fine-tuned. Table I shows the fine-tuned model's classification results after being trained on the different image types exemplified in Figure 4. The table also lists the model's training accuracy in paratheses. The table shows a clear divide between the classification statistics using original (no additional filters), gray, and HSV images and the Sobel XY, Edge (Canny edge detection), and threshold (canny edge detection with a lower threshold) images. The high classification statistics represent the ease in which the model accurately predicted the validation dataset, however, the values were likely high due to a lack of diversity between the training and validation images that contained the leak. Furthermore, a drop in precision and accuracy was observed when Sobel XY and edge detection images were used in the models. Those models did not learn valuable information for predicting the leak, rather they predicted the dominant class in an unbalanced dataset. Adding more images of leaks from other faults would allow the model to more accurately identify a leak rather than over-train on a single instance as well as allow for a more balanced training dataset.

Contrary to the classification statistics, the highest training accuracy was measured when HSV images were implemented into the model. This suggests that by shifting from the original RGB scale to a HSV scale, the model could more effectively learn the training set and thereby potentially provide useful information in future analyses.

Table I. Classification statistics for the model's predictions on the validation dataset. The training accuracies are in paratheses.

Image Type	Accuracy	Precision	Recall	F1 score
Original	1.00 (0.961)	1.00	1.00	1.00
Gray	1.00 (0.859)	1.00	1.00	1.00
HSV	0.977 (0.988)	1.00	0.97	0.985
Sobel XY	0.77 (0.75)	0.77	1.00	0.87
Edge	0.75 (0.56)	0.75	1.00	0.86
Threshold	0.77 (0.56)	0.77	1.00	0.87

Grad-CAM++ was then used to determine how the classification model made its prediction and what portions of the images were its focus. Grad-CAM++ mapped class activations from the final convolutional layer back to the input image, as seen in Figure 5. On the left image in Figure 5, the class activations were observed in a pixelated heatmap. This heatmap was then overlayed on the input image to visualize where the model's focus was in making its classification. In the right image of Figure 5, the overlayed heatmap showed that the model was focusing primarily on the contactor motor. These results are promising because the leak occurred at the tubing connection to the contactor motor.

If the model was focusing on the background or supporting fixtures (shown in the edges of the image), that would indicate that the model is learning based on irrelevant information or artifacts found in the background. These results showed that the color scaling related to changes in the hottest temperature measured between images, was not affecting the model's classification.

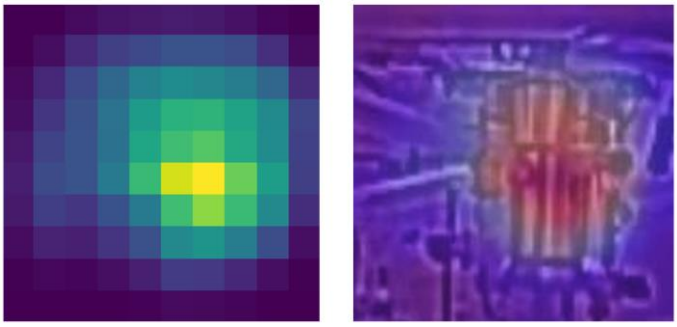

Figure 5. Heatmap created using Grad-CAM++ which maps the activations of the last convolutional layer of the classification algorithm to the input image (left). The heatmap is overlayed onto the input image shows that the algorithm focused on the contactor and not the background (right).

CONCLUSIONS

An assessment of sensors not typically installed in a solvent extraction process, that uses centrifugal contactors, is being conducted at Idaho National Laboratory. The research is being performed to inform the design of Beartooth; a testbed intended to study chemical separation processes specifically for the separation of usable and waste materials from used nuclear fuel. Signals from a variety of disparate sensors are being evaluated to determine if ML methods can identify features characteristic of equipment usage, process conditions, and other relevant information valuable to a process operator. The work includes monitoring solvent extraction equipment and solution flow with an infrared camera.

The infrared camera detected heated solution flowing to initially empty contactors through connective tubing. The results showed that an infrared camera could be used to inform a process operator of non-functioning equipment, blocked tubes, and the progression of solution through the system. This information could ultimately be used to improve the operation of a process.

A leak occurred during the progression of aqueous solution to additional contactors in the series of contactors. Infrared images were taken while the leak was occurring and were examined post process. Results from a ML classification model showed that the model was over-training due to the examination of data from only one leak. Although the results showed that the model was focused on a contactor within the images, it was difficult to ascertain whether the ML algorithm was focused on the correct aspects of the contactor.

Experiments, mimicking leaks, are being planned that would provide more data to process. In anticipation of this, a higher-resolution infrared camera has been acquired to capture additional system details. The ML methods described in this paper will be tested on data collected from the planned experiments.

REFERENCES

1. Paiva, A.P. and P. Malik, *Recent advances on the chemistry of solvent extraction applied to the reprocessing of used nuclear fuels and radioactive wastes.* Journal of Radioanalytical and Nuclear Chemistry, 2004. **261**(2): p. 485-496.
2. Irish, E.R., *DESCRIPTION OF PUREX PLANT PROCESS*. 1959, Hanford Atomic Products Operation, General Electric Company: United States.

3. Baumgärtner, F. and D. Ertel, *The Modern Purex Process and its Analytical Requirements.* Journal of Radioanalytical Chemistry, 1980. **58**: p. 11-28.
4. Modolo, G., et al., *A review of the demonstration of innovative solvent extraction processes for the recovery of trivalent minor actinides from PUREX raffinate.* Radiochimica Acta, 2012. **100**(8-9): p. 715-725.
5. Madic, C., et al., *Separation of long-lived radionuclides from high active nuclear waste.* Comptes Rendus Physique, 2002. **3**(7-8): p. 797-811.
6. Taylor, R.J., et al., *Progress towards the Full Recovery of Neptunium in an Advanced PUREX Process.* Solvent Extraction and Ion Exchange, 2013. **31**(4): p. 442-462.
7. Nash, K.L., et al., *Actinide Separation Science and Technology,* in *The Chemistry of the Actinide and Transactinide Elements*, L.R. Morss, N.M. Edelstein, and J. Fuger, Editors. 2011, Springer Netherlands: Dordrecht. p. 2622-2798.
8. Nash, K.L. and G.J. Lumetta, *Advanced Separation Techniques for Nuclear Fuel Reprocessing and Radioactive Waste Treatment*. Woodhead Publishing.
9. Regalbuto, M.C., et al., *Solvent extraction process development for partitioning and transmutation of used fuel*. 2005, NEA: Organisation for Economic Co-Operation and Development - Nuclear Energy Agency, Paris (France); Organisation for Economic Co-Operation and Development - Nuclear Energy Agency, 75 - Paris (France). Medium: X; Size: page(s) 373-385.
10. NEA, *Potential Benefits and Impacts of Advanced Nuclear Fuel Cycles with Actinide Partitioning and Transmutation*. 2011: Paris.
11. Poinssot, C., et al., *Main Results of the French Program on Partitioning of Minor Actinides, a Significant Improvement Towards Nuclear Waste Reduction.* Procedia Chemistry, 2012. **7**: p. 358-366.
12. Koch, L., *Minor actinide transmutation—a waste management option.* Journal of the Less Common Metals, 1986. **122**: p. 371-382.
13. Hou, X. and P. Roos, *Critical comparison of radiometric and mass spectrometric methods for the determination of radionuclides in environmental, biological and nuclear waste samples.* Analytica Chimica Acta, 2008. **608**(2): p. 105-139.
14. Bryan, S.A., et al., *Spectroscopic monitoring of used nuclear fuel reprocessing streams: an evaluation of used fuel solutions via Raman, visible, and near-infrared spectroscopy.* Radiochimica Acta, 2011. **99**(9): p. 563-572.
15. Tse, P., et al., *Review of on-line and near real-time spectroscopic monitoring of processes relevant to nuclear material management.* Analytica Chimica Acta, 2020. **1107**: p. 1-13.
16. Lines, A.M., et al., *Sensor Fusion: Comprehensive Real-Time, On-Line Monitoring for Process Control via Visible, Near-Infrared, and Raman Spectroscopy.* ACS Sensors, 2020. **5**(8): p. 2467-2475.
17. Nee, K., et al., *Combinations of NIR, Raman spectroscopy and physicochemical measurements for improved monitoring of solvent extraction processes using hierarchical multivariate analysis models.* Analytica Chimica Acta, 2018. **1006**: p. 10-21.
18. Padial-Collins, N.T., et al., *Centrifugal Contactors: Separation of an Aqueous and an Organic Stream in the Rotor Zone,* in *Separation Science and Technology*. 2006. p. 1001-1023.
19. Sharrad, C.A. and D.M. Whittaker, *7 - The use of organic extractants in solvent extraction processes in the partitioning of used nuclear fuels,* in *Reprocessing and Recycling of Used Nuclear Fuel*, R. Taylor, Editor. 2015, Woodhead Publishing: Oxford. p. 153-189.
20. Cárdenas, E.S., et al., *An Overview in the Development of a Multi-Sensor Data Science System for Monitoring a Solvent Extraction Process*, in *Proceedings of the INMM 63rd Annual Meeting*. 2022.
21. Hix, J.D., Cárdens, E.S., Ocampo Giraldo, L.A., *Multi-Sensor Data Acquisition System for Process Monitoring*, in *2022 ANS Winter Meeting and Technology Expo*. 2022: Phoenix, AZ.
22. Laboratory, I.N., *Deep Lynx: Digital Engineering Integration Hub*. 2022, Github.

23. Laboratory, I.N. *Computing Platforms: Deep Lynx*. [cited 2022; Available from: https://dice.inl.gov/computing-platforms/.
24. Hema, D. and S. Kannan, *Interactive Color Image Segmentation using HSV Color Space.* Science and Technology Journal, 2019. **7**(1).
25. Joblove, G.H. and D. Greenberg, *Color spaces for computer graphics.* ACM SIGGRAPH Computer Graphics, 1978. **12**(3): p. 20-25.
26. Vijayarani, S. and M. Vinupriya, *Performance Analysis of Canny and Sobel Edge Detection Algorithms in Image Mining.* International Journal of Innovative Research in Computer and Communication Engineering, 2013. **1**(8).
27. Basu, M., *Gaussian-based edge-detection methods-a survey.* IEEE Transactions on Systems, Man, and Cybernetics, Part C (Applications and Reviews), 2002. **32**(3): p. 252-260.
28. Chollet, F. *Xception: Deep Learning with Depthwise Separable Convolutions*. in *2017 IEEE Conference on Computer Vision and Pattern Recognition (CVPR)*. 2017.
29. Russakovsky, O., et al., *ImageNet Large Scale Visual Recognition Challenge.* International Journal of Computer Vision, 2015. **115**(3): p. 211-252.
30. Chattopadhay, A., et al. *Grad-CAM++: Generalized Gradient-Based Visual Explanations for Deep Convolutional Networks*. in *2018 IEEE Winter Conference on Applications of Computer Vision (WACV)*. 2018.

ACKNOWLEDGEMENTS

We are grateful to process operators who aided in the setup and operation of equipment. This research was funded through a Laboratory Directed Research and Development project under Battelle Energy Alliance, LLC contract number DE-AC07-05ID14517.